

A FINITE-DIFFERENCE APPROXIMATION TO NEWTON METHOD'S JACOBIAN MATRICES

Ruy M.O. Pauletti, Edgard S. Almeida Neto

*Polytechnic School of the University of São Paulo, P.O. Box 61548, 05424-970 São Paulo, Brazil,
<http://www.poli.usp.br>*

Keywords: Newton's Method, Numerical Methods, Nonlinear analysis.

Abstract. Newton's Method, the most widely used and robust tool for the solution of systems of nonlinear algebraic equations, requires successive evaluations of the Jacobian matrix, whose columns can be seen as the directional derivatives of the system's residual vector, with respect to each of its degrees of freedom. By their turn, these directional derivatives can be conveniently approximated by finite-difference schemes. However, a naïve application of such idea to solve large order nonlinear algebraic equations would easily compromise its practical attractiveness, because the number of required algebraic operations grows with the square of the order of the system.

In this paper, we consider problems where the residual vector is defined by sub-domains (or 'elements'), allowing the definition of element Jacobian matrices (of much smaller order than the global one), whose columns are again approximated by central-differences. So proceeding, the residual vector becomes locally supported, the global Jacobian matrix becomes sparse-banded, and much less numerical operations are required, since the number of operations in this case grows only linearly with order of the system.

Although the proposed finite-difference scheme implies in additional computational costs, if compared to the use of explicit formulas for the Jacobian matrices, its generality, simplicity and easy implementation encourages its use, whenever exact Jacobian matrices are not readily available. It can also be useful during the development of new families of finite elements, whose behavior can be quickly tested, before any consistent linearization of the residual vector is performed.

We have tested the proposed finite-difference approximation in problems of geometrically non-linear equilibrium of cable, membrane and shell structures, of elastic behavior, whose residual vectors and exact Jacobian matrices were already available in two different academic finite element programs, allowing quick performance assessments.

We have found out that the proposed approximate Jacobian matrices yield the same convergence rate and precision as the exact ones, with fairly acceptable extra computational costs. We defer a more comprehensive evaluation of relative computing costs to future papers, but we advance the notion that as the size of the problem is increased, the extra cost due to the proposed approximation becomes relatively smaller, whilst for small problems, the extra cost is relatively irrelevant.

1 INTRODUCTION

A broad class of problems of practical interest requires the numerical solution of a system of nonlinear algebraic equations, in the form of finding a *configuration vector* \mathbf{x}^* such that

$$\mathbf{g}(\mathbf{x}^*) = \mathbf{0}, \quad (1)$$

where $\mathbf{g}(\mathbf{x})$ is an "error" or *residual vector*.

We assume that vector \mathbf{x} spans a given *configuration space*, or *domain* Ω , over which the residual vector $\mathbf{g}(\mathbf{x})$ is well defined. In solid mechanics, for instance, in a Lagrangean description, \mathbf{x} is a vector of spatial coordinates spanning a given body Ω and $\mathbf{g}(\mathbf{x})$ is a vector of unbalanced forces defined all over the body.

Equation (1) can be solved –within a vicinity of the solution \mathbf{x}^* , supposing its existence– iterating Newton's recurrence formula,

$$\mathbf{x}_{k+1} = \mathbf{x}_k - \left(\frac{\partial \mathbf{g}}{\partial \mathbf{x}} \Big|_{\mathbf{x}_k} \right)^{-1} \mathbf{g}(\mathbf{x}_k) = \mathbf{x}_k - (\mathbf{J}_k)^{-1} \mathbf{g}(\mathbf{x}_k), \quad (2)$$

where we define the *Jacobian matrix*

$$\mathbf{J} = \frac{\partial \mathbf{g}}{\partial \mathbf{x}} = \left[\frac{\partial g_i}{\partial x_j} \right], \quad i, j = 1 \dots n_{dof}. \quad (3)$$

For recurrence (2) to work, \mathbf{J} must be a non-singular square matrix, of order n_{dof} , the number of degrees of freedom of the system.

We can partition the Jacobian matrix into columns, according to

$$\mathbf{J} = \left[\mathbf{j}_1 \quad \mathbf{j}_2 \quad \dots \quad \mathbf{j}_{n_{dof}} \right], \quad (4)$$

where \mathbf{j}_j are the *directional derivatives* of \mathbf{g} with respect to each component (or "degree of freedom") of \mathbf{x} :

$$\mathbf{j}_j = \frac{\partial \mathbf{g}}{\partial x_j} = \lim_{h \rightarrow 0} \left(\frac{\mathbf{g}(\mathbf{x} + h\boldsymbol{\delta}_j) - \mathbf{g}(\mathbf{x})}{h} \right), \quad j = 1 \dots n_{dof}, \quad (5)$$

where h is a scalar parameter and $h\boldsymbol{\delta}_j$ are perturbations of the j^{th} degree of freedom of the system, such that $\boldsymbol{\delta}_j = [\delta_i]$, $i = 1 \dots n_{dof}$, with $\delta_j = 1$, when $i = j$, and $\delta_i = 0$, when $i \neq j$.

The n_{dof} directional derivatives \mathbf{j}_k can be approximated by finite difference schemes. Considering a central-difference scheme, we have

$$\tilde{\mathbf{j}}_j = \frac{1}{2h} \left[\mathbf{J}(\mathbf{x} + h\boldsymbol{\delta}_j) - \mathbf{J}(\mathbf{x} - h\boldsymbol{\delta}_j) \right], \quad j = 1 \dots n_{dof}, \quad (6)$$

where now h is a finite scalar parameter and $\pm h\delta_j$ are backward and forward perturbations the j^{th} degree of freedom of the system.

Finally, inserting approximations \tilde{J}_j into (4), we obtain an approximate Jacobian matrix \tilde{J} , which can replace the exact Jacobian J in Newton's recurrence formula (2).

The numerical performance of such approximate Jacobian matrix \tilde{J} can at best match the performance provided by the exact Jacobian J , and resents from convergence problems similar to those displayed by the "exact" Newton's Method. Furthermore, perturbations $\pm h\delta_j$ resent from the lack of an obvious criterion for the magnitude of h affecting different degrees of freedom.

Although such type of finite-difference procedures have been already devised in the context of nonlinear inelastic solid mechanics, to compute approximate consistent tangent moduli, relating stress and strain ratios according to $\dot{\sigma} = \tilde{D}\epsilon$, for complicated material laws $\sigma = \sigma(\epsilon)$ (Miehe, 1995), (Pérez-Foguet *et al.*, 2000a/b, 2001), (Fellin and Ostermann, 2002), the order of the involved matrices in such problems is rather small.

For the overall equilibrium problem of large order systems,, a naïve application of such a scheme to Equation (1) easily compromises its practical attractiveness, because the number of required algebraic operations grows with the square of n_{dof} .

2 AN ELEMENT-WISE APPROXIMATION TO THE JACOBIAN MATRIX

In this paper, we are interested in the still broad class of problems where the residual vector g can be computed in sub-domains Ω^e , or finite elements, as a function of the *element configuration vectors* $x^e = [x_\alpha^e]$, where $e=1, \dots, n^e$, and n^e is the number elements, whilst $\alpha=1, \dots, n_\alpha^e$, and n_α^e is the number of nodes defining the e^{th} element. Defined onto every element, there exist an *element residual vector* $g^e = [g_\alpha^e]$, where $g_\alpha^e = g_\alpha^e(x^e)$ is the contribution of the e^{th} element to the residual vector evaluated at its α^{th} node.

We partition the *global configuration vector* according to $x = [x_1^T \ x_2^T \ \dots \ x_{n^e}^T]^T$, and observe that the element configuration vectors x^e can be extracted from the global one according to $x^e = A^e x$, where A^e is a Boolean *incidence matrix* for that element.

Likewise, the global residual vector and the global Jacobian matrix can be assembled according to

$$g = \sum_{e=1}^{n^e} A^{eT} g^e \tag{7}$$

and

$$J = \sum_{e=1}^{n^e} A^{eT} J^e A^e, \tag{8}$$

where we define the *element Jacobian matrix*

$$\mathbf{J}^e = \frac{\partial \mathbf{g}^e}{\partial \mathbf{x}^e} = \begin{bmatrix} \frac{\partial g_i^e}{\partial x_j^e} \end{bmatrix}, \quad i, j = 1, \dots, n_{dof}^e, \quad (9)$$

and n_{dof}^e denotes the number of degrees of freedom of the e^{th} element. Usually, $n_{dof}^e \ll n_{dof}$.

Of course, it is not convenient to perform the matrix multiplications implied in expressions (7) and (8), being quite more economical to add the element contributions directly to the global residual vector and Jacobian matrix, as explained in standard finite element textbooks.

Once again we partition the element Jacobian matrices according to

$$\mathbf{J}^e = \mathbf{J}^e(\mathbf{u}^e) \begin{bmatrix} \vdots & \vdots & \dots & \vdots \\ \vdots & \vdots & \dots & \vdots \\ \vdots & \vdots & \dots & \vdots \\ \vdots & \vdots & \dots & \vdots \end{bmatrix}, \quad (10)$$

where we define the *directional derivatives* of \mathbf{g}^e with respect to each element degree of freedom:

$$\mathbf{j}_j^e = \frac{\partial \mathbf{g}^e}{\partial x_j^e} = \lim_{h \rightarrow 0} \left(\frac{\mathbf{g}^e(\mathbf{x}^e + h\boldsymbol{\delta}_j^e) - \mathbf{g}^e(\mathbf{x}^e)}{h} \right), \quad j = 1, \dots, n_{dof}^e. \quad (11)$$

Likewise, we approximate these n_{dof}^e directional derivatives \mathbf{j}_j^e , by central-differences, according to

$$\tilde{\mathbf{j}}_j^e = \frac{1}{2h^e} \left[\mathbf{g}^e(\mathbf{x}^e + h^e\boldsymbol{\delta}_j^e) - \mathbf{g}^e(\mathbf{x}^e - h^e\boldsymbol{\delta}_j^e) \right], \quad j = 1, \dots, n_{dof}^e, \quad (12)$$

where h^e is a finite scalar parameter and $\pm h^e\boldsymbol{\delta}_j^e$ are backward and forward perturbations of the k^{th} element degree of freedom, such that $\boldsymbol{\delta}_j^e = [\delta_i]$, $i = 1, \dots, n_{dof}^e$, with $\delta_j = 1$, when $i = j$, and $\delta_i = 0$, when $i \neq j$.

Finally, inserting approximations $\tilde{\mathbf{j}}_j^e$ into (10), we obtain approximate element Jacobian matrices $\tilde{\mathbf{J}}^e$, $e = 1, \dots, n_{el}$, which are then assembled into a global approximate Jacobian matrix $\tilde{\mathbf{J}}$, according to (8).

An element-wise approximation naturally adapts h^e to the assumed mesh refinement, presumably well adjusted to the problem. The global residual vector becomes locally supported, since for every node, only the elements connected to the node need to be spanned. Likewise, the global stiffness matrix becomes sparse-banded, and much less numerical operations are required by element-wise perturbations since, as n_{dof} grows, the constant number of operations required by element-wise perturbations becomes relatively smaller than the number of operation of global perturbations. Besides, the overall number of operations grows only linearly with the number of elements. However, we defer a more precise evaluation on the numerical cost of these schemes to a future paper.

This element-wise scheme can provide surprisingly good approximations for the element Jacobian matrices \mathbf{J}^e , as long as h^e is limited to a fraction of the smaller element size, *i.e.*,

$$h^e \leq \varphi d^e \quad (13)$$

where d^e is the diameter of the inscribed circle (or another convenient measure of the smallest size of the element) and where the magnitude of φ depends on how sensible is \mathbf{g}^e , to perturbations affecting \mathbf{x}^e . In solid mechanics, for instance, φ would relate to the strains imposed to the element, by relative displacements among its nodes.

Although the number of the required perturbation operations will probably imply in additional computational costs, if compared to the use of explicit formulas for \mathbf{J}^e , the generality of the proposed approximation encourages its use whenever the Jacobian matrices are not readily available, for instance in cases where the residual vector is not fully analytically defined (such as in contact problems, for instance), or in cases where its consistent linearization is deemed too complicated to be sought. Besides, its simplicity and easy implementation can be useful during the development of new families of finite elements, whose behavior can be quickly tested, before any consistent linearization of the residual vector is performed.

The proposed approximation is also useful in the context of dynamic analyses, where it can provide the basis for a quick estimative of the critical time-step for explicit time-integration schemes (as will be described in a forthcoming paper (Pauletti and Guirardi, 2011)). Furthermore, the vector nature of approximations $\tilde{\mathbf{J}}_j$ can be explored, when parallel processing is used, to alleviate their extra computational cost.

3 AN APPLICATION TO A CABLE-MEMBRANE STRUCTURE

In order to study the performance of the proposed approximation to the Jacobian matrices, we initially introduce the problem of geometrically non-linear equilibrium of cable-membrane structures. A straightforward way to derive algebraic equilibrium for cable assemblies consists in assimilating the cables to a sequence of straight segments working under axial stress only. Likewise, membrane surfaces can be approximated by a collection of plane triangular facets, under a plane stress state. So discretized, cables and membranes can be treated as **systems of central forces**, as depicted in Figure 1, where we consider that the nodal coordinates of such a system are stored in vectors $\mathbf{x}_\alpha = [\bar{x}_\alpha]$, $\alpha = 1, \dots$, by their turn collected into the *global position vector* $\mathbf{x} = [\mathbf{x}_1^T \quad \mathbf{x}_2^T \quad \dots \quad \dots^T]^T$.

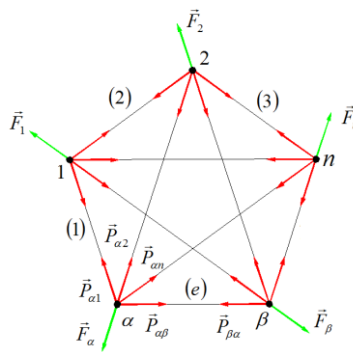


Figure 1: A system of n central forces

Each node has only displacement degrees-of-freedom $\mathbf{u}_\alpha = [\bar{u}_\alpha]$, which are stored in a *global displacement vector* $\mathbf{u} = [\mathbf{u}_1^T \quad \mathbf{u}_2^T \quad \dots \quad \dots^T]$. Similarly, The external loads acting on these nodes, $\mathbf{f}_\alpha = [\bar{F}_\alpha]$, are stored in a *global external load vector* $\mathbf{f} = [\mathbf{f}_1^T \quad \mathbf{f}_2^T \quad \dots \quad \dots^T]$, and the nodal force interactions $\mathbf{p}_\alpha = [\sum_{\beta=1}^n \bar{P}_{\alpha\beta}]$ are stored in a *global internal load vector* $\mathbf{p} = [\mathbf{p}_1^T \quad \mathbf{p}_2^T \quad \dots \quad \dots^T]$. The position vector can be written as $\mathbf{x} = \mathbf{x}^0 + \mathbf{u}$, where \mathbf{x}^0 is a constant vector which describes an initial configuration.

With the above definitions, the solution of the problem of equilibrium of a system of central forces consists in finding a displacement vector \mathbf{u}^* such that

$$\mathbf{g}(\mathbf{u}^*) = \mathbf{p}(\mathbf{u}^*) - \mathbf{f}(\mathbf{u}^*) = \mathbf{0}. \tag{14}$$

3.1 A straight cable element

We consider that cables are approximated by an assemblage of tension-only straight elements. Figure 2 depicts a generic, e^{th} element in a current configuration, with nodes indexed as α and β , in the global structural system, and as 1 and 2, in the element numeration system.

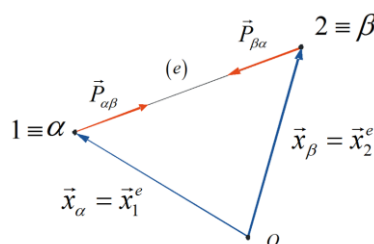


Figure 2: A truss element, with local and global nodal indexes

Keeping implicit the element index e , for basic quantities, we define the vector $\mathbf{l} = \mathbf{x}_2 - \mathbf{x}_1$, and the current element length is given by $\ell = \|\mathbf{l}\|$, whilst $\mathbf{v} = \mathbf{l}/\ell$ is the unit vector directed from node 1 to node 2. The element is described in an initial configuration, already under a normal force N^0 . Thus the reference, zero-stress element length, is given by $\ell = \ell^0 \sqrt{1 - \nu^0}$ and the normal force acting on the

element, at each instant, is given by $N = EA \left(\frac{\ell}{\ell} \right) \ell$, if $\ell \geq \ell$, or $N = 0$, when $\ell < \ell$, since a cable cannot withstand compression.

The *internal forces vector* for a truss element is given by

$$\mathbf{p}^e = \begin{bmatrix} -\mathbf{v} \\ \mathbf{v} \end{bmatrix} N = \mathbf{C}N, \quad (15)$$

where $\mathbf{C} = \begin{bmatrix} -\mathbf{v}^T & \mathbf{v}^T \end{bmatrix}^T$ is a *geometric operator*.

The contribution of a generic element defined by nodes $\{\alpha, \beta\}$ to the global internal load vector is given by Equation (7), with $\mathbf{A}_{1\alpha}^e = \mathbf{A}_{2\beta}^e = \mathbf{I}_3$ and $\mathbf{A}_{1m}^e = \mathbf{A}_{2m}^e = \mathbf{0}$, $m \in \{1, 2, \dots, n_n \setminus \{\alpha, \beta\}\}$, where $\mathbf{0}$ and \mathbf{I}_3 are, respectively, the null and identity matrices of order three, and n_n is the number of nodes of the whole structure.

Proceeding along some straightforward derivations, the *Jacobian*, or *tangent stiffness matrix* of the straight cable is obtained (dropping the index of the element to alleviate notation):

$$\mathbf{J}^e = \mathbf{k}_t = \frac{\partial \mathbf{p}}{\partial \mathbf{u}} = \frac{EA}{\ell} \mathbf{C} \mathbf{C}^T + \frac{N}{\ell} \begin{bmatrix} (\mathbf{I}_3 - \mathbf{w}^T) & -(\mathbf{I}_3 - \mathbf{w}^T) \\ \vdots & \vdots \\ (\mathbf{I}_3 - \mathbf{w}^T) & (\mathbf{I}_3 - \mathbf{w}^T) \end{bmatrix} = \mathbf{k}_e + \mathbf{k}_g, \quad (16)$$

where we have assumed that there is no contribution of the external force vector \mathbf{f} to the tangent stiffness. The components \mathbf{k}_e and \mathbf{k}_g stand for a *linear-elastic* and a *geometric stiffness matrix*, respectively. When $\ell = \ell$, we take $\mathbf{p}^e = \mathbf{0}$ and $\mathbf{k}_t = \mathbf{0}$. Once again, the contribution of every element to the global stiffness is given by Equation (8).

3.2 Argyris' Natural Membrane Finite Element

The Argyris' natural triangular membrane finite element allows also membranes to be treated as systems of central forces (Argyris, 1974), (Pauletti *et al.*, 2005), (Pauletti, 2008). Argyris element is defined in an *initial configuration* Ω^0 , in which it is already under a given stress field. A *reference configuration* Ω^r usually refers to stress-free conditions. The element's *current configuration* is denoted by Ω^c .

Element nodes and edges are numbered anticlockwise, with edges facing nodes of same number. Nodal coordinates are referred to a global Cartesian system, and a local coordinate system, indicated by an upper hat, is adapted to every element configuration, such that the \hat{x} axis is always aligned with edge 3, oriented from node 1 to node 2, whilst the \hat{z} axis is normal to the element plane.

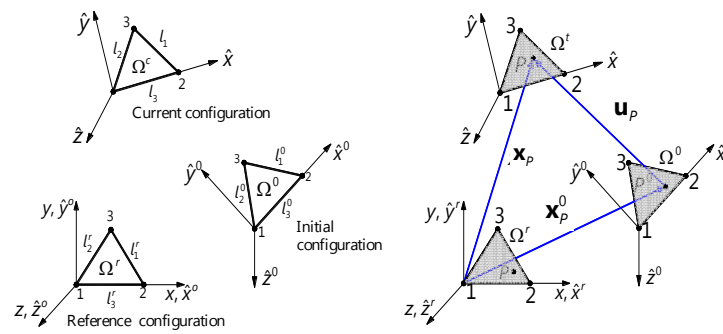


Figure 3: (a) A triangular element Ω^e in three different configurations; (b) position vector $\mathbf{x}_p = \mathbf{x}_p^0 + \mathbf{u}_p$

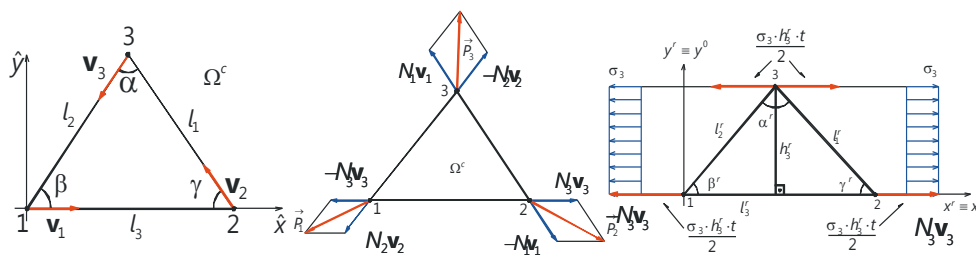


Figure 4: (a) Unit vectors \mathbf{v}_α , $\alpha = 1, 2, 3$, along the element edges; (b) internal nodal forces \mathbf{p}_α , decomposed into natural forces $N_\alpha \mathbf{v}_\alpha$; (c) determination of natural force N_3

Current global coordinates of the element nodes, are given by $\mathbf{x}_\alpha = \mathbf{x}_\alpha^0 + \mathbf{u}_\alpha$, $\alpha = 1, 2, 3$, where \mathbf{u}_i are the nodal displacements. The lengths of element edges are given by $l_\alpha = \|\mathbf{x}_\gamma - \mathbf{x}_\beta\|$, with indexes $\alpha, \beta, \gamma = 1, 2, 3$ in cyclic permutation. Unit vectors parallel to the element edges are denoted by $\mathbf{v}_\alpha = \mathbf{l}_\alpha / \|\mathbf{l}_\alpha\|$.

With these definitions, the vector of internal nodal forces can be decomposed into forces parallel to the element edges, according to

$$\mathbf{p}^e = \begin{bmatrix} \mathbf{p}_1 \\ \mathbf{p}_2 \\ \mathbf{p}_3 \end{bmatrix} = \begin{bmatrix} N_2 \mathbf{v}_2 - N_3 \mathbf{v}_3 \\ N_3 \mathbf{v}_3 - N_1 \mathbf{v}_1 \\ N_1 \mathbf{v}_1 - N_2 \mathbf{v}_2 \end{bmatrix} = \begin{bmatrix} \mathbf{0} & \mathbf{v}_2 & -\mathbf{v}_3 \\ -\mathbf{v}_1 & \mathbf{0} & \mathbf{v}_3 \\ \mathbf{v}_1 & -\mathbf{v}_2 & \mathbf{0} \end{bmatrix} \begin{bmatrix} N_1 \\ N_2 \\ N_3 \end{bmatrix} = \mathbf{C} \mathbf{N}, \quad (17)$$

where \mathbf{C} is a geometric operator, which collects the unit vectors parallel to the element edges and $\mathbf{N} = [N_1 \ N_2 \ N_3]^T$ is the vector of natural forces.

In order to avoid unnecessary complication, for the aim of this paper, we assume the behavior of the element is linear-elastic, and we avoid introducing any consideration of membrane wrinkling or slackening. Under such simplified assumptions, there exists a linear relationship

$$\mathbf{N} = \mathbf{k}_n \mathbf{a}, \quad (18)$$

where $\mathbf{a} = [\Delta l_\alpha \ l_\alpha \ l_\alpha^{-T}]$, is the vector of natural displacements (with $\Delta l_\alpha \ l_\alpha \ l_\alpha^{-T}$, $\alpha = 1, 2, 3$) and the element natural stiffness is a constant matrix given by

$$\mathbf{k}_n = V_r \mathcal{L}_r^{-1} \mathbf{T}_r^{-T} \hat{\mathbf{D}} \mathbf{T}_r^{-1} \mathcal{L}_r^{-1}, \tag{19}$$

where V_r is the element volume, $\mathcal{L}_r = \text{diag}\{\ell_{\dots}\}$, $\hat{\mathbf{D}}$ collects the coefficients of Hooke's law for plane stresses, such that $\hat{\boldsymbol{\sigma}} = \hat{\mathbf{D}} \hat{\boldsymbol{\varepsilon}}$ and, finally, \mathbf{T}_r is a transformation matrix, relating the linear Green strains $\hat{\boldsymbol{\varepsilon}}$ to the *natural strains* $\boldsymbol{\varepsilon}_n = \mathcal{L}_r^{-1} \mathbf{a}$, i.e., $\boldsymbol{\varepsilon}_n = \mathbf{T}_r \hat{\boldsymbol{\varepsilon}}$.

The vector of internal forces at each configuration is then given by

$$\mathbf{p}^e = \mathbf{C} \mathbf{k}_n \mathbf{a}. \tag{20}$$

It is interesting to define also an *external wind load vector* is also defined, according to

$$\mathbf{f}_w^e = -\frac{\rho A}{3} [\mathbf{I}_3 \quad \mathbf{I}_3 \quad \mathbf{I}_3]^T \mathbf{n}, \tag{21}$$

where ρ is a normal wind pressure acting on the element, A is its area and \mathbf{n} its normal unit vector, in the current configuration. The contributions of \mathbf{p}^e and \mathbf{f}_w^e to the global load vector are again given by (7), now with $\mathbf{A}_{1\alpha}^e = \mathbf{A}_{2\beta}^e = \mathbf{A}_{3\gamma}^e = \mathbf{I}_3$ and $\mathbf{A}_{1m}^e = \mathbf{A}_{2m}^e = \mathbf{A}_{3m}^e = \mathbf{O}$, $m \in \{1, 2, \dots, \dots, \beta, \gamma\}$.

Proceeding with derivations, the *Jacobian*, or *tangent stiffness matrix* of the membrane element is obtained (once again, dropping the index of the element to alleviate notation):

$$\begin{aligned} \mathbf{J}^e &= \mathbf{k}_t = \frac{\partial \mathbf{g}}{\partial \mathbf{u}} \\ &= \mathbf{C} \mathbf{k}'_n \mathbf{C}^T + \begin{bmatrix} \left(\frac{N_2}{\ell} \mathbf{M} + \frac{N_3}{\ell} \mathbf{M} \right) & -\frac{N_3}{\ell} \mathbf{M} & -\frac{N_2}{\ell} \mathbf{M} \\ -\frac{N_3}{\ell} \mathbf{M} & \left(\frac{N_1}{\ell} \mathbf{M} + \frac{N_3}{\ell} \mathbf{M} \right) & -\frac{N_1}{\ell} \mathbf{M} \\ -\frac{N_2}{\ell} \mathbf{M} & -\frac{N_1}{\ell} \mathbf{M} & \left(\frac{N_1}{\ell} \mathbf{M} + \frac{N_2}{\ell} \mathbf{M} \right) \end{bmatrix} + \frac{\rho}{6} \begin{bmatrix} \boldsymbol{\Lambda}_1 & \boldsymbol{\Lambda}_2 & \boldsymbol{\Lambda}_3 \\ \boldsymbol{\Lambda}_1 & \boldsymbol{\Lambda}_2 & \boldsymbol{\Lambda}_3 \\ \boldsymbol{\Lambda}_1 & \boldsymbol{\Lambda}_2 & \boldsymbol{\Lambda}_3 \end{bmatrix} \\ &= \mathbf{k}_e + \mathbf{k}_g + \mathbf{k}_{ext} \end{aligned} \tag{22}$$

where $\mathbf{M}_1 = \mathbf{I}_3 - \mathbf{v}_1 \mathbf{v}_1^T$; $\mathbf{M}_2 = \mathbf{I}_3 - \mathbf{v}_2 \mathbf{v}_2^T$; $\mathbf{M}_3 = \mathbf{I}_3 - \mathbf{v}_3 \mathbf{v}_3^T$ and where $\boldsymbol{\Lambda}_\alpha = \text{skew}(\mathbf{I}_\alpha)$, $i = 1, 2, 3$, are skew-symmetric matrices, whose axial vectors are given by $\mathbf{l}_\alpha = \ell_{\dots}$, and where each component define, respectively, the *elastic*, the *geometric* and the *external components* of the *tangent stiffness matrix*.

It is seen that \mathbf{k}_g , for a natural membrane element, is analogous to the geometric stiffness of a closed assemblage of three geometrically exact truss elements, under normal loads N_α . It is also seen that $\mathbf{k}_{ext} = \frac{\partial \mathbf{f}}{\partial \mathbf{u}}$ is an asymmetric matrix, reflecting the fact that wind loads are generally non-conservative. However, inspection of \mathbf{k}_{ext} shows that non-symmetric terms cancel out for adjacent elements, and thus, for any assemblage of elements under a constant pressure and borders fully constrained, the global \mathbf{K}_t is symmetric, and the system is conservative.

3.3 A first numerical application

The elements describe above were already implemented in the SATS program, developed in the MATLAB programming environment (Pauletti *et al.*, 2005), (Pauletti, 2008). We have used this program to implement approximate Jacobian matrices $\tilde{\mathbf{c}}$ for both cable and membrane elements, and applied it to the analysis of a rough model of a saddle membrane bordered by cables and fixed vertices.

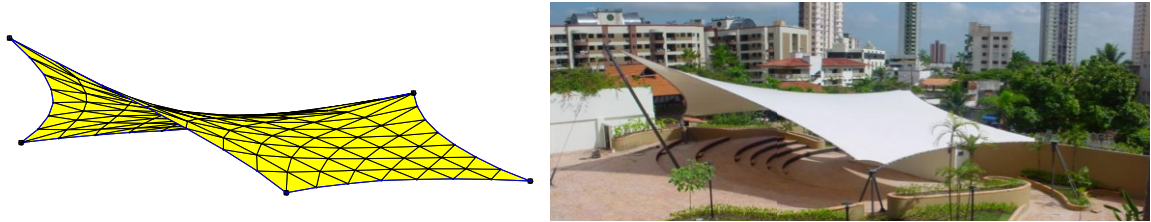


Figure 5: The membrane roof of the "Memorial dos Povos de Belém do Pará"

The model shown in Figure 5(a) corresponds to a simplified version of the models used to design an actual structure, the "Memorial dos Povos de Belém do Pará" (shown in Figure 5(b)), which has been used in several occasions as a benchmark to test different analysis methods and computer programs, with excellent agreement of independent results (Pauletti and Brasil, 2005), (Pauletti *et al.*, 2009), (Pauletti and Martins, 2009). Figure 6(a) shows a top view of the mesh, which can be inscribed in a rectangle 28.64m long by 22.59m wide. The mesh has 120 nodes, with 196 membrane elements and 42 cable elements. We considered a membrane with elastic modulus $E=1\text{ GPa}$ and thickness $t=1\text{ mm}$, under a uniform and isotropic initial stress field $\sigma_0=5\text{ MPa}$, whilst border cables had an axial stiffness modulus $EA=0.1\text{ GPa}$, under initial normal loads $N_0=100\text{ kN}$.

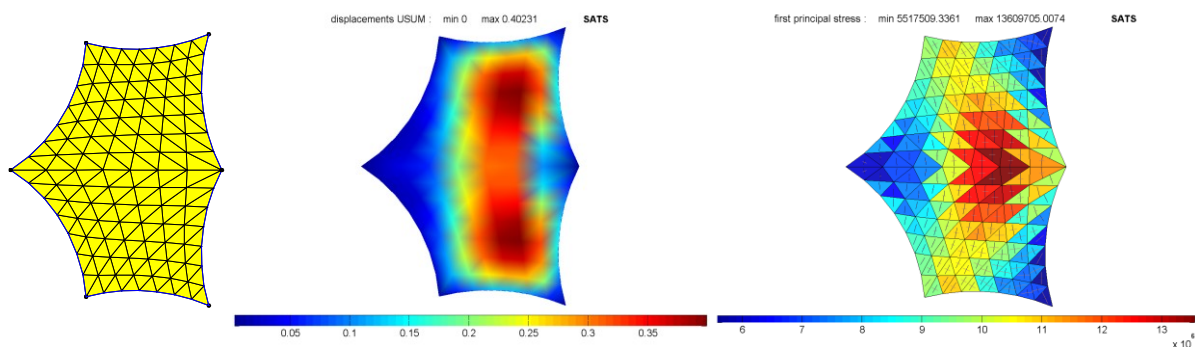


Figure 6: (a) a top view of the finite element mesh; (b) field of displacement norms (in meters); (c) 1st principal stresses σ_1 (in N/m^2)

Figure 6(b) shows the field of displacement norms under a uniform upward wind load $q=286\text{ N/m}^2$, acting over the whole membrane surface. Figure 6(c) shows the field of the 1st principal stresses over the membrane. Precisely the same numerical

results were obtained both with the exact Jacobian \mathbf{J} or the approximate Jacobian $\tilde{\mathbf{J}}$ matrices (up to the chosen precision), but the number of iterations required for convergence depended on the magnitude of perturbation $h^e = \varphi d^e$, where d^e was considered equal to the minimum element height.

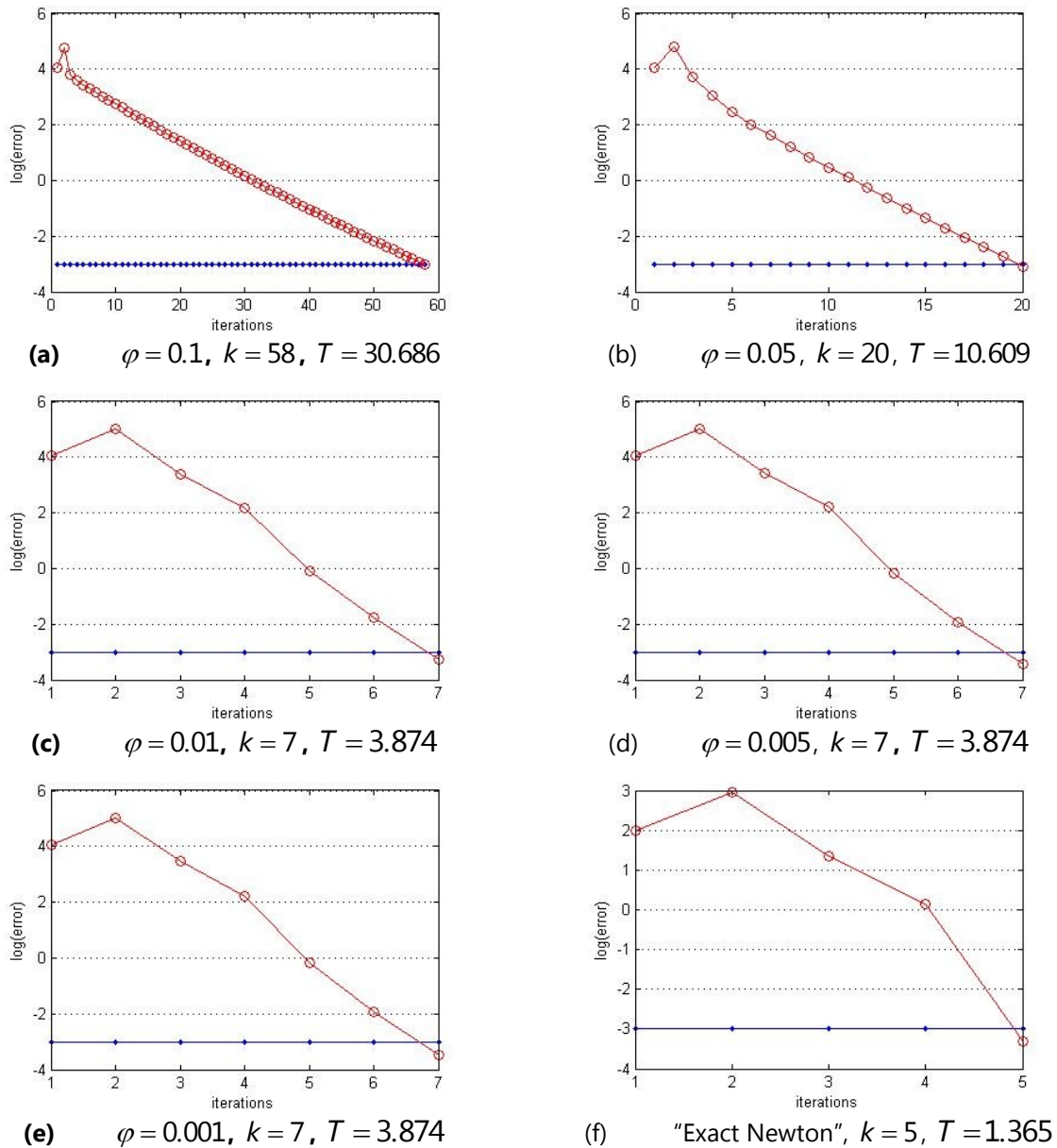


Figure 7: Variation of the residual norm $\varepsilon = \|\mathbf{g}\|$ for different φ values

(k, T): (number of iterations and computation time required to achieve convergence, in seconds)

Figures 7(a) to 7(e) show the variation of the *residual norm* $\varepsilon = \|\mathbf{g}\|$, for solution using the approximate Jacobian matrix $\tilde{\mathbf{J}}$, considering different values for the scalar parameter φ . We have assumed $\varepsilon_{lim} = 10^{-3}$ N as the criterion for convergence. Figure 7(f) shows the variation of the residual norm, for solution using the exact Jacobian matrix \mathbf{J} . Also given in Figures 7(a) to 7(f) are the different number of iterations k and

times T required to achieve convergence.

It is seen that the number of iterations required for convergence is reduced as φ is diminished. It is also seen that the average iteration time using the approximate Jacobian matrix $\tilde{\mathbf{J}}$ (0.54 seconds), is equal to twice the average time using the exact Jacobian matrix \mathbf{J} (0.27 seconds), and is independent from the magnitude of φ .

These results suggest that, although the use of exact Jacobian matrices \mathbf{J} is computationally more efficient, solution can also be achieved using the proposed approximate matrices $\tilde{\mathbf{J}}$, yielding the same precision with an acceptable extra computational cost, provided that φ is kept small enough.

The finite-difference approximation of the Jacobian matrices proposed in this paper can also provide the basis for a quick estimative of the critical time step of conditionally-stable time integration schemes, in the context of explicit dynamic analysis, based on the maximum eigenvalues of the elements' stiffness matrices. Figure 8 shows the values of the larger eigenvalues of membrane and cable elements of the models studied above, considering matrices \mathbf{J}^e and $\tilde{\mathbf{J}}$. Membrane elements are numbered from 1 to 196, and cable elements range from 197 to 238. There are slight asymmetries in the tangent stiffness matrices of membrane elements, due to the influence of pressure loads. We considered only the real part of their eigenvalues. It is seen that estimatives for the maximum element eigenvalues, considering either \mathbf{J}^e or $\tilde{\mathbf{J}}$ are practically superimposed, even if quite rough values for the scalar parameter φ are taken.

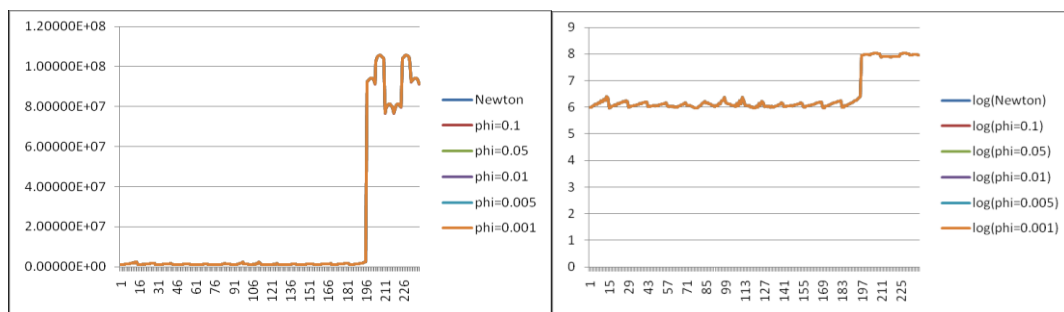


Figure 8: Variation of the maximum eigenvalues of membrane and cable elements: (a) linear scaling; (b) the same, in logarithmic scaling

4 AN APPLICATION TO A SHELL FINITE ELEMENT

As a second example, still in the field of structural mechanics, we have applied the proposed $\tilde{\mathbf{J}}$ approximation to the triangular shell element originally developed by Campello *et al.* (2003). Shell elements provide interesting benchmarks to our procedure, because they involve different types of degrees of freedom. Moreover, since both the *unbalanced force vector* and the *consistent tangent stiffness matrix* (or the residual vector and the exact Jacobian matrix, in the terminology of our paper) are available for this element, once again a direct confrontation of results obtained

through the proposed approximations $\tilde{\cdot}$ or the exact Jacobian matrices \mathbf{J}^e is possible.

The chosen element is a displacement-based triangular shell with 6 nodes, derived from a fully nonlinear six parameter (3 displacements and 3 rotations) shell model for finite deformations, where finite rotations are treated by the *Euler-Rodrigues* formula. The element has a nonconforming linear rotation field but compatible quadratic interpolation for the displacements. Figure 9 shows the basic kinematical description used in the model, as well as the element in reference and deformed configurations.

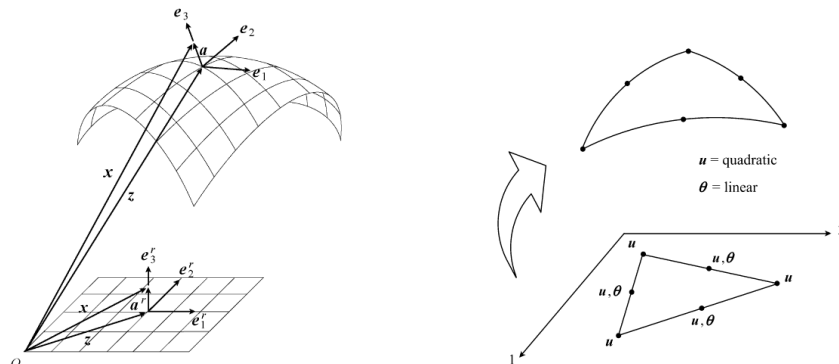


Figure 9: Kinematical description and the element in reference and deformed configurations. Adapted from Campello *et al.* (2003)

After a lengthy derivation, Campello *et al.* arrived at the *vector of residual nodal forces*,

$$\mathbf{P}_e = \int_{\Omega_e} \left[\mathbf{N}^T \bar{\mathbf{q}} - (\Psi_\alpha \mathbf{N})^T \boldsymbol{\sigma}_\alpha \right] d\Omega \tag{23}$$

where \mathbf{N} is the matrix of element shape functions, $\bar{\mathbf{q}}$ is a generalized external force vector, given by

$$\bar{\mathbf{q}} = \begin{bmatrix} \bar{\mathbf{n}} \\ \mathbf{\Gamma}^T \bar{\mathbf{m}} \end{bmatrix}, \quad \bar{\mathbf{n}} = \mathbf{t}^t + \mathbf{t}^b + \int_H \mathbf{b} d\zeta, \quad \bar{\mathbf{m}} = \mathbf{a}^t \times \mathbf{t}^t + \mathbf{a}^b \times \mathbf{t}^b + \int_H \mathbf{a} \times \mathbf{b} d\zeta \tag{24}$$

and $\bar{\mathbf{n}}, \bar{\mathbf{m}}$ are the applied external forces and moments, both per unit area of the middle surface in the reference configuration, whilst \mathbf{t} is the surface traction and \mathbf{b} is the body forces, both per unit reference volume, and upper indexes t and b refer to the shell top and bottom surfaces.

Also, $\boldsymbol{\sigma}_\alpha$ is a vector of generalized cross-sectional internal forces, given by

$$\boldsymbol{\sigma}_\alpha = \begin{bmatrix} \mathbf{n}_\alpha^r \\ \mathbf{m}_\alpha^r \end{bmatrix}, \quad \mathbf{n}_\alpha^r = \int_H \boldsymbol{\tau}_\alpha^r d\zeta, \quad \mathbf{m}_\alpha^r = \int_H \mathbf{a}^r \times \boldsymbol{\tau}_\alpha^r d\zeta, \tag{25}$$

and $\mathbf{n}_\alpha^r, \mathbf{m}_\alpha^r$ are back-rotated cross-sectional forces and moments, both per unit length, and $\boldsymbol{\tau}_\alpha^r$ is a back-rotated stress vectors acting on the cross-sections of the element reference configuration.

Finally Ψ_α is a matrix operator fully described by Campello *et al.*, which also

presents the consistent tangent stiffness matrix for this shell, given by

$$\mathbf{k}_e = \int_{\Omega_e} \left[(\boldsymbol{\Psi}_{\alpha\mathbf{N}})^T \mathbf{D}_{\alpha\beta} (\boldsymbol{\Psi}_{\beta\mathbf{N}}) + (\boldsymbol{\Delta}_{\alpha\mathbf{N}})^T \mathbf{G}_{\alpha} (\boldsymbol{\Delta}_{\alpha\mathbf{N}}) - \mathbf{N}^T \mathbf{L} \mathbf{N} \right] d\Omega \quad (26)$$

which involves several other matrix operators, also defined in the paper.

Once again, contributions of every element to the global residual vector and to the global Jacobian matrix are assembled considering Equations (7) and (8), with conveniently defined Boolean operators \mathbf{A}^e .

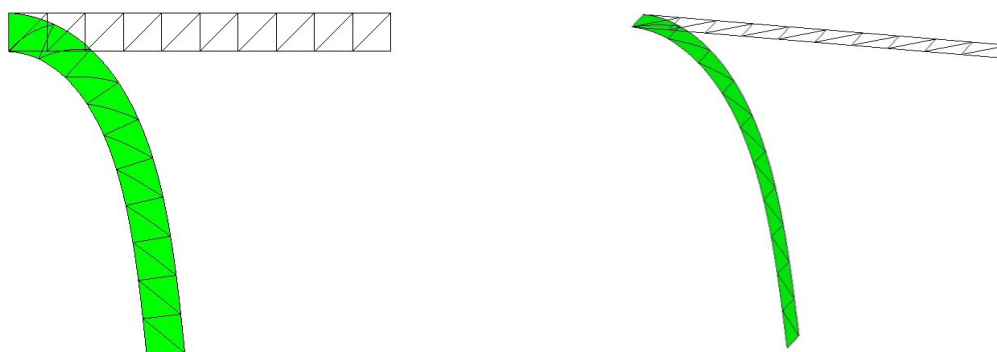
4.1 A second numerical application

The above summarized shell element is implemented in the program PEFSYS, an academic finite element code first presented in Pimenta *et al.* (1998). We have used PEFSYS to implement approximate Jacobian matrices $\tilde{\mathbf{J}}$ for this element, and applied it to Example 2 of Campello *et al.* (2003).

As in the case of cables and membranes, in order to obtain a central finite-difference approximation $\tilde{\mathbf{J}}$, we introduce perturbations $\pm h\boldsymbol{\delta}_j$ into the vector of residual nodal forces, Equation (23). For perturbation of the displacements degrees of freedom, we once again assume that $h_u = \varphi d^e$, where d^e is equal to the minimum height of the triangular element, and φ can be interpreted as a strain value. On the other hand, for the rotational perturbations, obtained by dividing a transversal perturbation by d^e , we have simply $h_\theta = \varphi$, where now φ can be seen as a small rotation.

We studied a cantilever beam of squared cross-section subjected to a large point load at the center of its free end. An elastic modulus $E = 10^7$ Pa and a Poisson coefficient $\nu = 0.3$ are assumed, with a length $L = 1.0$ m and a square cross-section $0.1\text{m} \times 0.1\text{m}$. Two different situations were enforced: (i) in-plane bending, with a load $P = 1000\text{N}$ at the free end and on the same plane of the beam and (ii) out-of-plane bending with the same load applied to the free end, but in the out-of-plane direction.

Figure 10 shows the deformed shape obtained for both situations, using either the exact Jacobian matrices \mathbf{J}^e , given by Equation (26), or the approximate Jacobian matrices $\tilde{\mathbf{J}}$ (Equations (10) and (12)), with $\varphi = 0.0001$. Results for the tip deflection, for either procedures and for both situations (i) and (ii), are in strict adherence to those presented by Campello *et al.* (2003), which by their turn adhere to other independent investigations on the same problem (Simo *et al.*, 1991), (Wriggers and Gruttmann, 1993).



(i) in-plane bending

(ii) out-of-plane bending

Figure 10: Deformed shapes for the second example

Table 1 compares the *axial* (u) and *in-plane transversal* (w) components of the free end displacement (node 62 of the model) for the in-plane bending model, obtained using either the exact Jacobian matrix \mathbf{J} or the approximate Jacobian matrices $\tilde{\mathbf{J}}$, for increasing values of vertical load at this same node. Total adherence between results is observed, up to the displayed precision.

| Node62 | Solution using \mathbf{J} | | Solution using $\tilde{\mathbf{J}}$ | |
|--------|-----------------------------|--------------|-------------------------------------|--------------|
| Load | U | W | U | W |
| 100 | -0.75525E-01 | -0.34863E+00 | -0.75525E-01 | -0.34863E+00 |
| 200 | -0.19835E+00 | -0.54491E+00 | -0.19835E+00 | -0.54491E+00 |
| 300 | -0.29837E+00 | -0.64843E+00 | -0.29837E+00 | -0.64843E+00 |
| 400 | -0.37358E+00 | -0.70923E+00 | -0.37358E+00 | -0.70923E+00 |
| 500 | -0.43095E+00 | -0.74884E+00 | -0.43095E+00 | -0.74884E+00 |
| 600 | -0.47598E+00 | -0.77683E+00 | -0.47598E+00 | -0.77683E+00 |
| 700 | -0.51227E+00 | -0.79785E+00 | -0.51227E+00 | -0.79785E+00 |
| 800 | -0.54220E+00 | -0.81441E+00 | -0.54220E+00 | -0.81441E+00 |
| 900 | -0.56738E+00 | -0.82792E+00 | -0.56738E+00 | -0.82792E+00 |
| 1000 | -0.58891E+00 | -0.83928E+00 | -0.58891E+00 | -0.83928E+00 |

Table 1: axial (u) and in-plane transversal (w) components of the free end displacement, for the in-plane bending model

Similarly, Table 2 compares the *axial* (u) and *out-of-plane transversal* (w) components of the free end displacements, for the out-plane bending model. Once again, total adherence is observed between results obtained using either the exact Jacobian matrix \mathbf{J} or the approximate Jacobian matrix $\tilde{\mathbf{J}}$.

| Node62 | Solution using \mathbf{J} | | Solution using $\tilde{\mathbf{J}}$ | |
|--------|-----------------------------|--------------|-------------------------------------|--------------|
| Load | U | W | U | W |
| 100 | -0.76532E-01 | -0.35105E+00 | -0.76532E-01 | -0.35105E+00 |
| 200 | -0.20049E+00 | -0.54794E+00 | -0.20049E+00 | -0.54794E+00 |
| 300 | -0.30111E+00 | -0.65155E+00 | -0.30111E+00 | -0.65155E+00 |
| 400 | -0.37662E+00 | -0.71237E+00 | -0.37662E+00 | -0.71237E+00 |
| 500 | -0.43418E+00 | -0.75203E+00 | -0.43418E+00 | -0.75203E+00 |
| 600 | -0.47931E+00 | -0.78007E+00 | -0.47931E+00 | -0.78007E+00 |
| 700 | -0.51568E+00 | -0.80115E+00 | -0.51568E+00 | -0.80115E+00 |
| 800 | -0.54568E+00 | -0.81777E+00 | -0.54568E+00 | -0.81777E+00 |
| 900 | -0.57091E+00 | -0.83134E+00 | -0.57091E+00 | -0.83134E+00 |
| 1000 | -0.59248E+00 | -0.84277E+00 | -0.59248E+00 | -0.84277E+00 |

Table 2: axial (u) and out-of-plane transversal (w) components of the free end displacement, for the out-of-plane bending model

Finally, Table 3 compares the global residual norms ($\varepsilon = \|\mathbf{g}\|$) for both the in-plane and out-of-plane bending situation. For every load increment, values obtained after the first Newton iteration and after convergence are presented, using either the exact Jacobian matrix \mathbf{J} or approximate Jacobian matrix $\tilde{\mathbf{J}}$.

For either procedure, numerical results were precisely the same (up to the displayed precision), therefore not repeated in the table. Also the number of iterations required to achieve convergence at every load step was exactly the same, showing that, at least in this particular case, the use of the approximate Jacobian matrix $\tilde{\mathbf{J}}$ does not degrade the convergence of Newton's Method.

We defer a more comprehensive evaluation of relative computing costs to future papers. However, we have observed that due to a larger number of algebraic operations required to assemble the approximate Jacobian matrix $\tilde{\mathbf{J}}$, the total processing time to solve our second example using them was about 10 times the total time required by exact Jacobian matrix \mathbf{J} . However, generally speaking, the ratio of the assembling time to the total solution time usually decreases, as the number of degrees of freedom grows, thus becoming less determinant of total computing cost. We have solved our second example also with 1000 elements (still a small problem size), and the ratio of total processing time, required by $\tilde{\mathbf{J}}$ or \mathbf{J} , dropped to 3:1. Thus, it seems that in most practical application, the extra cost implied in assembling $\tilde{\mathbf{J}}$ instead of \mathbf{J} should be acceptable, either because the problem size is small (thus extra costs are irrelevant) or because the problem size is large enough to the assembling time become relatively small, compared to the total solution time.

| Load | Iter | $\varepsilon = \ \mathbf{g}\ $ for \mathbf{J} | $\varepsilon = \ \mathbf{g}\ $ for $\tilde{\mathbf{J}}$ |
|------|------|---|---|
| 100 | 1 | 230.542546244211 | 230.543656770391 |
| | 7 | 1.304558361945308E-011 | 3.799264612338969E-011 |
| 200 | 1 | 66.1596496678850 | 66.1503188394626 |
| | 9 | 2.650522980730921E-005 | 2.675853163502189E-005 |
| 300 | 1 | 16.1395386834461 | 16.1403326155677 |
| | 6 | 2.044304568923653E-009 | 1.931809180526349E-009 |
| 400 | 1 | 4.78913832449426 | 4.78982206802382 |
| | 5 | 5.742312024310899E-009 | 6.013474615731024E-009 |
| 500 | 1 | 1.75602666611174 | 1.75628799118380 |
| | 4 | 1.369119066987591E-007 | 1.374524109032094E-007 |
| 600 | 1 | 0.762420833867086 | 0.762522899787127 |
| | 4 | 8.606667109289488E-009 | 8.438045594823579E-009 |
| 700 | 1 | 0.378542580585105 | 0.378587203503452 |
| | 4 | 4.252131491947199E-010 | 4.092036061435904E-010 |
| 800 | 1 | 0.209630281403916 | 0.209652198777477 |
| | 4 | 2.547937528631010E-011 | 2.569215096310905E-011 |
| 900 | 1 | 0.127006854344617 | 0.127018739005226 |
| | 4 | 2.575370602543687E-012 | 3.374867274764152E-012 |
| 1000 | 1 | 8.282253489881622E-002 | 8.282953298553968E-002 |
| | 3 | 6.894725385753278E-009 | 6.325943712886397E-009 |

Table 3: Residual Norms, for either in-plane and out-of-plane bending models

5 CONCLUSIONS

In this paper, we consider geometrically nonlinear problems where the residual vector is defined by sub-domains (or 'elements'), allowing the definition of element Jacobian matrices, in such a way that the residual vector becomes locally supported, the global Jacobian matrix becomes sparse-banded, and much less numerical operations are required, since the number of operations in this case grows only linearly with order of the system.

Although the proposed finite-difference scheme implies in additional computational costs, if compared to the use of explicit formulas for the Jacobian matrices, its generality, simplicity and easy implementation encourages its use, whenever exact Jacobian matrices are not readily available. It can also be useful during the development of new families of finite elements, whose behavior can be quickly tested, before any consistent linearization of the residual vector is performed.

We have tested the proposed finite-difference approximation in problems of geometrically non-linear equilibrium of cable, membrane and shell structures, of elastic behavior, whose residual vectors and exact Jacobian matrices were already available in two different academic finite element programs, allowing quick performance assessments.

We have found out that the proposed approximate Jacobian matrices yield the same convergence rate and precision as the exact ones, with fairly acceptable extra computational costs. We defer a more comprehensive evaluation of relative computing costs to future papers, but we advance the notion that as the size of the problem is increased, the extra cost due to the proposed approximation becomes relatively smaller, whilst for small problems, the extra cost is relatively irrelevant.

REFERENCES

- Argyris J.H., Dunne P.C., Angelopoulos, T., Bichat B., Large natural strains and some special difficulties due to non-linearity incompressibility in finite elements. *Comp. Meth. Appl. Mech. Eng.* 4 (2), 219–278, 1974.
- Campello, E.M.B., Pimenta, P.M. and Wriggers, P., A triangular finite shell element based on a fully nonlinear shell formulation, *Computational Mechanics* 31 (2003) 505–518.
- Fellin, W. and Ostermann, A., Consistent tangent operators for constitutive rate equations, *Int. J. Numer. Anal. Meth. Geomech.* 26 (2002) 1213–1233.
- Miehe, C., Numerical computation of algorithmic (consistent) tangent moduli in large-strain computational inelasticity. *Computer Methods in Applied Mechanics and Engineering* 134 (1996) 223–240.
- Pauletti R.M.O., Guirardi D.M. and Deifeld T.E.C., Argyris' Natural Membrane Finite element Revisited. *Textile Composites and Inflatable Structures*, Barcelona, CIMNE, 335-344, 2005.
- Pauletti R.M.O and Brasil R.L.M.R.F., Structural Analysis and Construction of the

- Membrane Roof of the "Memorial dos Povos de Belém do Pará". *II Simposio Latinoamericano de Tensoestructuras*, Caracas, 2005.
- Pauletti R.M.O., Static Analysis of Taut Structures. *Textile Composites and Inflatable Structures II*. Dordrecht: Springer-Verlag, 117-139, 2008.
- Pauletti R.M.O., Guirardi D.M. and Gouveia S., Modeling sliding cables and geodesic lines through dynamic relaxation, *IASS Symposium*, Valence, 2009.
- Pauletti, R.M.O. and Martins, C.B., Modeling the slippage between membrane and border cables, *IASS Symposium*, Valence, 2009.
- Pauletti, R.M.O. and Guirardi, D.M. An Efficient Mass-Tuning Algorithm for the Dynamic Relaxation Method. To be presented at the *V International Conference on Textile Composites and inflatable Structures (Membranes 2011)*, October 2011, Barcelona, Spain.
- Pérez-Foguet, A., Rodríguez-Ferran, A. and Huerta, A., Numerical differentiation for non-trivial consistent tangent matrices: an application to the MRS-Lade model, *Int. J. Numer. Meth. Engrg* 48 (2000) 159-184.
- Pérez-Foguet, A., Rodríguez-Ferran, A. and Huerta, A., Numerical differentiation for local and global tangent operators in computational plasticity, *Comput. Methods Appl. Mech. Engrg.* 189 (2000) 277-296.
- Pérez-Foguet, A., Rodríguez-Ferran, A. and Huerta, A., Consistent tangent matrices for substepping schemes, *Comput. Methods Appl. Mech. Engrg.* 190 (2001) 4627-4647.
- Pimenta, P.M., Maffei, C.E.M., Gonçalves, H.H., Pauletti, R.M.O., A Programming system for nonlinear dynamic and static analysis of tall buildings, *Proceedings of the IV World Congress on Computational Mechanics*, Buenos Ayres, 1998.
- Simo J.C., Fox D.D., Rifai M.S., On a stress resultant geometrically exact shell model. Part III: computational aspects of the nonlinear theory, *Comput. Meth. Appl. Mech. Eng.* 79: 21-70 (1990).
- Wriggers P., Gruttmann, F., Thin shells with finite rotations formulated in Biot stresses: theory and finite element formulation, *Int. J. Numer. Meth. Eng.* 36: 2049-2071 (1993)